Available online at www.sciencedirect.com
ScienceDirect
Ceramics International 35 (2009) 77–81
CERAMICS INTERNATIONAL
www.elsevier.com/locate/ceramint

# Effect of thermal treatment on the electrical properties of the sol–gel-derived (Zr,Sn)$TiO_4$ thin films

Ru-Yuan Yang [a], Hon Kuan [b], Min-Hang Weng [c,*], Yung-Shou Ho [d]

[a] *Department of Materials Engineering, National Ping-Tung University of Science and Technology, Taiwan*
[b] *Department of Technology Electro-Optical Engineering, Southern Taiwan University of Technology, Taiwan, ROC*
[c] *National Nano Device Laboratories, Taiwan*
[d] *Department of Applied Chemistry, Fooyin University, Taiwan*

Received 13 March 2007; received in revised form 27 August 2007; accepted 22 September 2007
Available online 8 December 2007

**Abstract**

The effect of heating temperatures on the electrical properties of sol–gel-derived (Zr,Sn)$TiO_4$ thin films deposited on a p-type (1 0 0) Si substrate was studied. The leakage currents of films with two different heating temperatures chosen to burn-out the solvent as a function of applied voltage were measured at different temperatures. The activation energies obtained from the Arrhenius plot of the leakage current density versus measured temperature for (Zr,Sn)$TiO_4$ films were then extracted. Additionally, microstructures of films with two different heating temperatures chosen to burn-out the solvent were analyzed by a conductive atomic force microscope (AFM) and an X-ray diffraction (XRD). Finally, the conductive mechanisms of leakage current and leakage current correlated to microstructures were also discussed.


*Keywords:* $(Zr_{0.8},Sn_{0.2})TiO_4$; Leakage current; Microstructure; Thin film; Sol–gel

## 1. Introduction

There is a continued trend in miniaturization of conventional integrated circuits (ICs) and microwave monolithic integrated circuits (MMICs), without compromising the efficiency. This has prompted an upsurge in the quest for alternative dielectric thin films to conventional $SiO_2$. Hence, high dielectric constant materials have been attractive candidates for gate dielectrics, dynamic random access memories (DRAMs) and microwave communications applications [1,2]. Metal oxides, such as zirconium oxide ($ZrO_2$), hafnium oxide ($HfO_2$), and tantalum oxide ($Ta_2O_5$), are potential candidates for this purpose [3–5]. However, most of the high-*k* films suffer from a high leakage current after being processed at a high temperature [4].

$ZrTiO_4$ with 20 mol% Zr replaced by Sn ions has proved to be one of the most popular high dielectric materials for microwave devices [6,7]. Most $ZrTiO_4$-based thin films prepared by RF sputtering [8–12] or pulse laser ablation [13,14] with high physical power in the deposition process induce the formation of the interface layer and high surface roughness. Sol–gel process is a simple and inexpensive chemical route to fabricate the nano-powders and thin films [15,16]. The process can coat huge surface even with odd geometry without using expensive vacuum systems. However the control of the process parameters is critical in making a good homogeneity and crack free of the film. In a previous work, a sol–gel-derived $(Zr_{0.8}Sn_{0.2})TiO_4$ (abbreviated as ZST) thin films have been prepared and the processing conditions on the microstructure were discussed. However, the effect of heating temperatures on the relationships between the microstructure and the leakage currents were not reported [16].

In this paper, the effect of heating temperatures chosen to burn-out the solvent on the microstructure and the leakage currents were studied. The relationships between the microstructure and the leakage currents were discussed. Additionally, the activation energies obtained from the Arrhenius plot of ln *J*/*E* versus 1000/*T* for ZST films were extracted. Finally, the leakage current densities correlated to microstructures were also discussed.

* Corresponding author. Tel.: +886 6 5050650; fax: +886 6 5050553.
*E-mail address:* mhweng@mail.ndl.org.tw (M.-H. Weng).

0272-8842/$34.00 
doi:10.1016/j.ceramint.2007.09.108

## 2. Experimental procedure

High-purity zirconium oxychloride ($ZrOCl_2{\cdot}8H_2O$, 99.99%), stannic chloride ($SnCl_4{\cdot}5H_2O$, 99.99%) and tetrabutyl titanate ($Ti(OC_4H_9)_4$, 99.99%) were used as starting materials and methanol was used as solvent for the precursors to control viscosity and cracking of the thin film. Metal ratios in the precursor mixtures were Zr:Sn:Ti (in molar ratio) = 4:1:5. The precursor solutions were mixed and refluxed at 68 °C for 3 h. Solution was spin-coated directly on p-type (1 0 0) Si wafers with resistivity of 3–10 Ω cm. The wafers were washed carefully before coating according to standard RCA method to form a uniform wet film at room temperature. Two different heating temperatures, 250 °C and 450 °C used to burn-out the organic compounds were chosen as the processing parameters in this process using the differential thermal analysis (DTA) (not shown) [16]. The samples with different heating temperatures of 250 °C and 450 °C are named as samples A and B, respectively. The heating rate of the furnace was 10 °C/min and the sample surround in the atmosphere during thermal treatment process. These above two steps were repeated several times and the films were finally annealed in air at 700 °C for a total of 30 min to crystallize the amorphous films. The procedure flow chart was shown in Fig. 1. The detail procedure and the relationship between the thickness and the coating layer can be found in a previous paper of the Ref. [16].

In this study, the average film thicknesses of samples A and B used to be analyzed are 135 nm and 100 nm, respectively. Crystalline structure of the ZST films were identified by a rotating X-ray diffraction (XRD) using Cu Kα radiation (wavelength is 0.15418 nm), and surface microstructures and surface morphologies of the thin films were analyzed by a conductive atomic force microscope (AFM). Several Al top electrodes with an area of $1.22 \times 10^{-3}\ cm^2$ were sputter deposited on the top surface of ZST films through a metal shadow mask to form MIS capacitors. The leakage current densities of the ZST film versus electric field characteristics were measured using the computer-controlled HP 4156 by applying dc voltages with a step height of 1 V and a delay time of 30 s. The leakage current measurements were carried out in the measured temperature range of 50–125 °C.

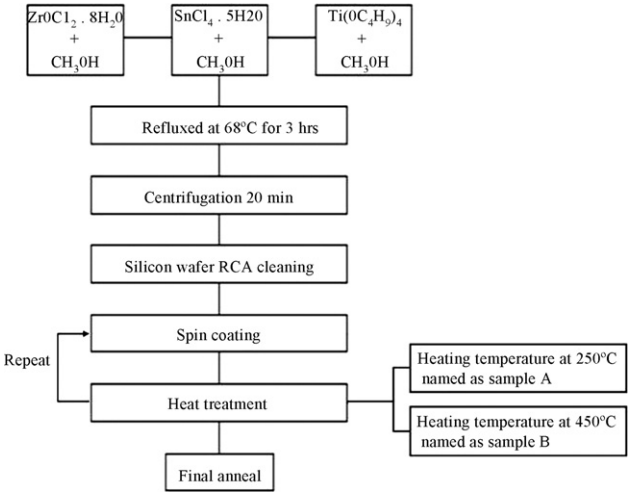


Fig. 1. The flow chart to prepare ZST thin films.

## 3. Result and discussions

### 3.1. Effect of heating temperatures on the microstructures

Fig. 2 displays XRD patterns of ZST films for sample A and sample B. The films contain crystalline phase corresponding to orthorhombic ZST with (1 1 1), (1 1 0) and (0 0 2) orientations, which are well consistent with the ZST pattern found in JCPDS of 81-2214. The level of crystallinity and the crystal sizes of the films are determined by the diffraction peak widths. With lower heating temperature (sample A) such as at 250 °C, the films showed more intense diffraction peaks, indicating a greater volume percentage of crystalline phases. For higher heating temperature (sample B) such as at 450 °C, the full width at half maximum (FWHM) of the $2\theta_{(1\ 1\ 1)}$ peaks increased, indicating finer crystal grains and higher concentration of crystal defects [9]. The averaged crystal size of ZST films for sample A and sample B are 23 nm and 8 nm, respectively, according to the XRD line broadening by using Scherrer formula [17].

Fig. 3 shows AFM top view of ZST films for sample A and sample B. The roughness of root mean square (RMS) of ZST film for samples A and B are 7 nm and 8.85 nm, respectively. It indicates that sample A has smoother surface than sample B. Although the sample A has larger crystal size than sample B (identified by XRD), in sample B (higher heating temperature), the solvent and organic compounds are removed more rapidly and violently to make the surface of sample B rougher than sample A [16].

### 3.2. Effect of heating temperatures on the electrical properties

Leakage current density is a critical issue of concern in memory device or gate dielectrics applications. Therefore, a current density ($J$)–electric field ($E$) relation was analyzed. Fig. 4 shows the leakage current densities of ZST films for

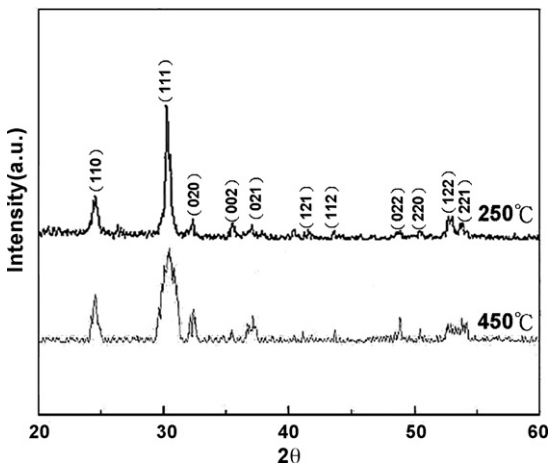


Fig. 2. XRD patterns of ZST films for sample A with heating temperature at 250°C and sample B with heating temperature at 450 °C.

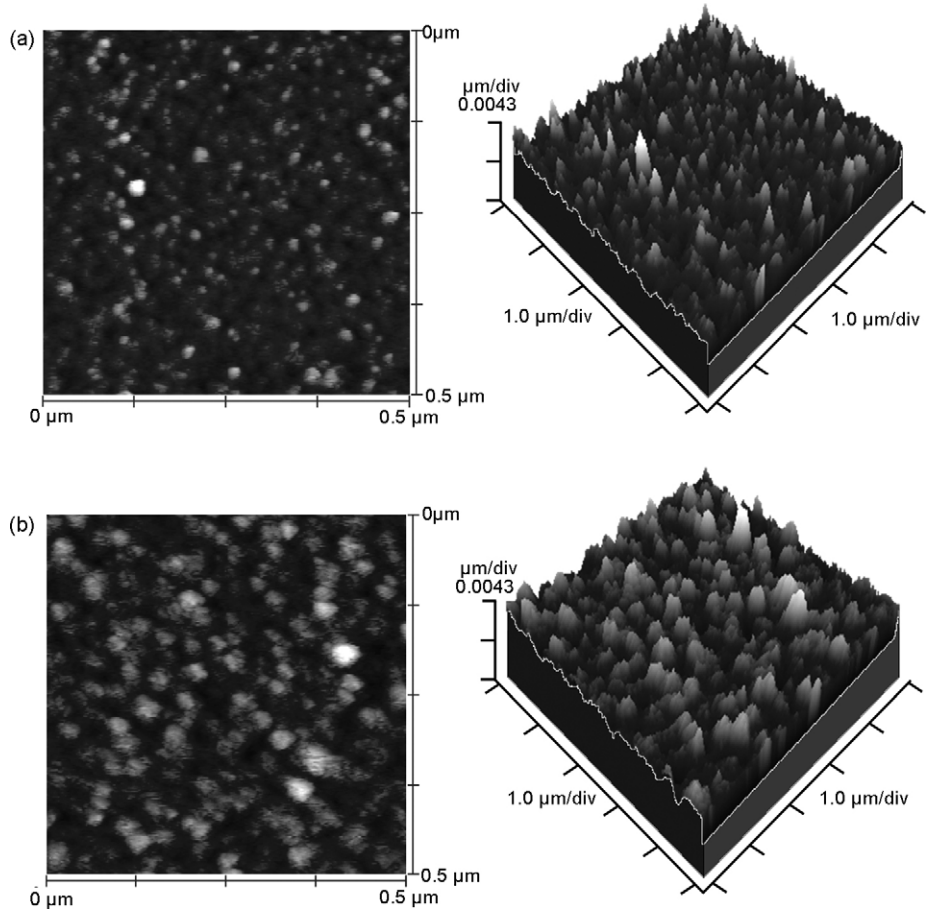


Fig. 3. AFM top view of ZST films for (a) sample A and (b) sample B.

samples A and B. The measured temperature is 100°C. The leakage current densities under direct current condition (dc) at the benchmark field of 1.5 MV/cm are $4.92 \times 10^{-8}$ A/cm$^2$ and $1.02 \times 10^{-7}$ A/cm$^2$ of ZST film for samples A and B, respectively. Although the sample B has higher leakage currents than that at sample A, the leakage currents of prepared ZST films are suitable for the target range for DRAM applications ($(1–5) \times 10^{-7}$ A/cm$^2$) [2].

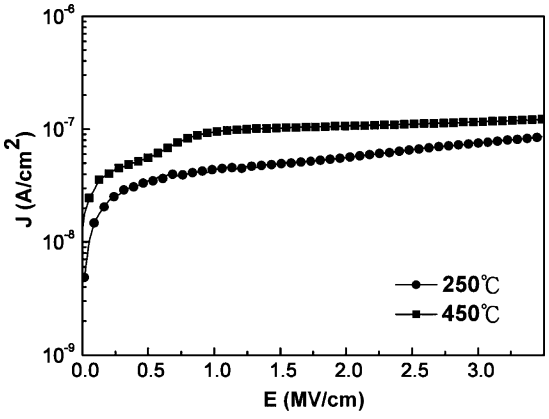


Fig. 4. The leakage current densities of ZST films for sample A (circle) and sample B (square). The measured temperature is 100 °C.

Fig. 5 displays the leakage current densities as functions of measured temperatures in ZST films of ZST films for samples A and B. The leakage current density of ZST thin films was measured on applying the gate voltage at different temperatures and measuring the current with a delay time of 1 s. In general, the leakage current densities increase with increase of the measured temperatures in both samples A and B. Not only sample A but also sample B reveal a strong temperature dependence, which leads us to believe that the conductive mechanism through the ZST dielectric layer is the field-enhanced thermal excitation of trapped charge carriers into the conduction band [18]. However, it is difficult to determine whether the leakage current flows through the grains or through the grain boundaries, although a learned presume would be that the largest fraction of the current is transported through the grain boundaries [18], since the prepared ZST film is polycrystalline.

### 3.3. Discussion of conductive mechanism

The degradation of electronic devices was resulted from the scaling down of the insulator on the Si substrate to make an increase in the electric field. To understand the transport phenomena on the carriers flow in dielectrics, there are various models including Schottky emission, Poole–Frenkel emission,

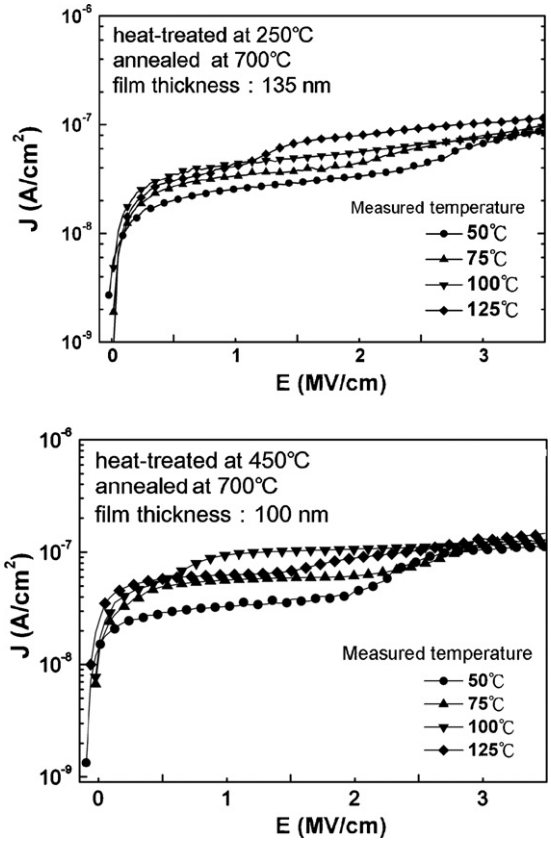


Fig. 5. The leakage current densities as functions of measured temperatures in ZST films for (a) sample A and (b) sample B.

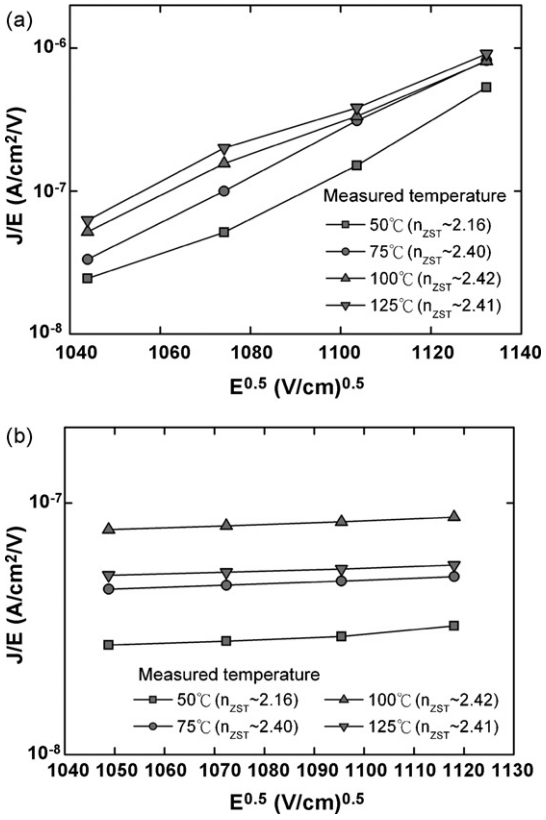


Fig. 6. The Poole–Frenkel plot of log ($J/E$) vs. $E^{1/2}$ under the negative bias of Al/ZST/p-Si capacitors for (a) sample A and (b) sample B.

Fowler–Nordheim tunneling, and a space charge limited current are used to evaluate the leakage currents in a dielectric film [19]. If the higher voltage regime such as an electric field larger than 50 kV cm$^{-1}$ was made, the Schottky and Poole–Frenkel mechanisms were analyzed. The lowering of a Coulombic potential barrier with the applied electric field is resulted in the Schottky (electrode limited conduction) and Poole–Frenkel (bulk limited conduction) effects. A relation of current density ($J$)–electric field ($E$) for the Schottky emission is given by the Schottky–Richardson relation.

$$J = AT^2 \exp\left[\frac{-q\varphi_o}{kT} + \frac{\beta_{sc}E^{1/2}}{kT}\right]$$

where $A$ is the Richardson–Dushman constant, $q$ represents the electronic charge, $T$ represents absolute temperature, $\varphi_o$ is the barrier height, $k$ is the Boltzmann constant and $\beta_{sc} = (q^3/4\pi\varepsilon_0 K_T)^{1/2}$ where $\varepsilon_0$ is the permittivity of free space, $K_T$ denotes the high-frequency dielectric constant and $n$ is the refractive index of the dielectrics. The ZST dielectric layer is believed as the Poole–Frenkel emission, more like as the field-enhanced thermal excitation [18]. The current density ($J$) related to the Poole–Frenkel emission can be expressed as follows:

$$J = CE \exp\left[\frac{-q\phi_t}{kT} + \frac{q\sqrt{qE/\pi\varepsilon_r\varepsilon_0}}{rkT}\right] \quad (1)$$

where $C$ is a constant, $E$ represents electric field, $T$ represents absolute temperature, $k$ is Boltzmann constant, $q$ denotes electronic charge, $q\phi_t$ is energy barrier height, $\varepsilon_0$ is the permittivity of free space, $\varepsilon_r$ is the high-frequency dielectric constant and $r$ is the coefficient which takes into account the influence of the trapping or acceptor centers ($1 \leqq r \leqq 2$) with $r = 1$ and $r = 2$ denoting the normal and modified Poole–Frenkel effects, respectively [18–20]. The high-frequency dielectric constant ($\varepsilon_r$) is given by the square of the refractive index $n$ ($\varepsilon_r = n^2$).

Therefore, the Poole–Frenkel plot of log ($J/E$) versus $E^{1/2}$ under the negative bias (accumulation region) for Al/ZST/p-Si MIS capacitors of ZST films for samples A and B are shown in Fig. 6(a) and (b), respectively. The calculated refractive index from the experimental curves agrees well with $n_{ZST}$ ($n_{ZST} \sim 2$–3) [15]. The normal Poole–Frenkel conduction mechanism describing the bulk limited charge transport was identified in the present sol–gel-derived ZST thin films.

### 3.4. Relationships between the microstructure and the leakage currents

Fig. 7 shows the ln $J/E$ versus 1000/$T$ at an electric field of 1 MV/cm of ZST films for samples A and B. The Poole–Frenkel (bulk limited conduction) mechanism results from the lowering of a Coulombic potential barrier with the applied electric field by the imperfect (defects or voids) in the dielectric and many grain boundaries forming the conduction paths. Since the curves match very well with the Frenkel–Poole electron emission equation, the result further supports the postulation

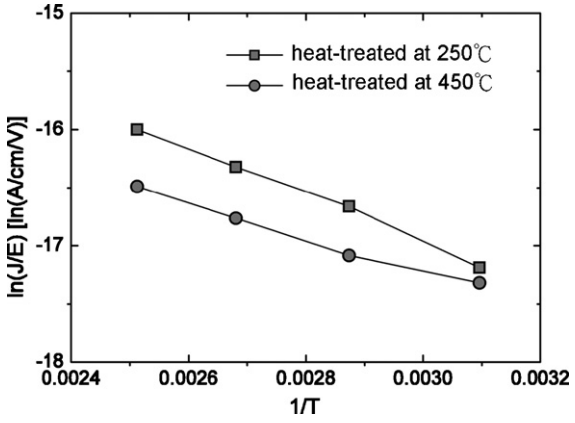


Fig. 7. ln *J/E* vs. 1000/*T* at an electric field of 1 MV/cm of ZST films for (a) sample A and (b) sample B.

that field-enhanced thermal excitation of trapped electrons into the conduction band is the major leakage mechanism [19]. The extracted activation energies obtained from the Arrhenius plot of ln *J/E* versus 1000/*T* at an electric field of 1 MV/cm of ZST films for samples A and B were 0.184 eV and 0.122 eV, respectively. The reason may be that sample B have a finer crystal size (more grain boundary) and higher concentration of defects observed by XRD analysis and more rough surfaces observed by AFM analysis, therefore rough interfaces, microvoids and the defect induce many charge trap energy levels to reduce trap activation energy of sample B. These activation energies are enough to represent the required excitation energies for the charge carriers to participate in the conduction mechanism from the shallow trap levels which are usually distributed near the conduction band edge of the material [20]. That is to say, the carriers in the sample with heating temperature of 250 °C (sample A) must get more energy to overcome the barrier to conduct than that of 450 °C (sample B). The lower activation energy of sample B correlated with microstructures exhibit a higher leakage current than sample A, as shown in Fig. 4.

## 4. Conclusion

In summary, the effect of heating temperatures on the electrical properties as well as microstructure of sol–gel-derived (Zr,Sn)$TiO_4$ thin films deposited on a p-type (1 0 0) Si substrate was investigated. ZST films with heating temperature at 250 °C (sample A) have larger grain size, lower concentration of defects and more smooth surface than those at 450 °C (sample B). As a result, films with heating temperature at 250 °C (sample A) have larger activation energy to participate in the conduction mechanism compared to films with heating temperature at 450 °C (sample B). It is found that the dominant mechanism responsible for conduction through the prepared ZST films is the field-enhanced thermal excitation of Poole–Frenkel model. The leakage current density of prepared ZST films is affected by microstructure as well as activation energies, but the values are acceptable to be suitable for application in electronic devices.

## Acknowledgements

The authors would like to acknowledge Mr. S.S. Wang of Fooyin University for preparing the samples and National Nano Device Laboratories (NDL) for supporting the material and electrical analyzing equipments.

## References

[1] M. Sze, Physics of Semiconductor Devices, John Wiley & Sons, New York, 1981.
[2] The International Technology for Semiconductor, Semiconductor Industry Association, Tokyo, Japan, 2004.
[3] Y. Kuo, J. Lu, J.Y. Tewg, Tantalum nitride interface layer influence on dielectric properties of hafnium doped tantalum oxide high dielectric constant thin films, Jpn. J. Appl. Phys. 42 (7A) (2003) L769–L771.
[4] J.Y. Tewg, Y. Kuo, J. Lu, B. Schueler, Electrical and physical characterization of zirconium-doped tantalum oxide thin films, Electrochem. Soc. 151 (3) (2004) F59–F67.
[5] R.F. Cava, W.F. Peck, J.J. Krajewski, Enhancement of the dielectric constant of $Ta_2O_5$ through substitution with $TiO_2$, Nature (London) 377 (1995) 215–217.
[6] H. Ikawa, A. Iwai, K. Hiruta, H. Shimojima, K. Urabe, S. Udagawa, Phase transformation and thermal expansion of zirconium and hafnium titanates and their solid solutions, J. Am. Ceram. Soc. 71 (2) (1988) 120–127.
[7] C.L. Huang, M.H. Weng, The microwave dielectric properties and the microstructures of Bi(Nb·Ta)$O_4$ ceramics, Jpn. J. Appl. Phys. 38 (10) (1999) 5949–5952.
[8] C.L. Huang, C.H. Hsu, Properties of reactively radio frequency-magnetron sputtered (Zr·Sn)$TiO_4$ dielectric films, J. Appl. Phys. 96 (2) (2004) 1186–1191.
[9] D.A. Chang, P. Lin, T.Y. Tseng, Effects of oxygen-argon mixing on the electrical and physical properties of $ZrTiO_4$ films sputtered on silicon at low temperature, J. Appl. Phys. 78 (12) (1995) 7103–7108.
[10] D.A. Chang, P. Lin, T.Y. Tseng, Growth of highly oriented $ZrTiO_4$ thin films by radio-frequency magnetron sputtering, Appl. Phys. Lett. 64 (24) (1994) 3252–3254.
[11] F.J. Wu, T.Y. Tseng, Highly oriented ($Zr_{0.7}Sn_{0.3}$)$TiO_4$ thin films grown by rf magnetron sputtering, J. Am. Ceram. Soc. 81 (2) (1998) 439–445.
[12] R.B. van Dover, L.F. Schneemeyer, Deposition of uniform Zr–Sn–Ti–O films by on-axis reactive sputtering, IEEE Electron Device Lett. 19 (9) (1998) 329–331.
[13] O. Nakagawara, Y. Toyota, M. Kobayashi, Y. Yoshino, Y. Katayama, H. Tabata, T. Kawai, Electrical properties of (Zr·Sn)$TiO_4$ dielectric thin film prepared by pulsed laser deposition, J. Appl. Phys. 80 (1) (1996) 388–392.
[14] P. Victor, S.B. Krupanidhi, Impact of microstructure on electrical characteristics of laser ablation grown $ZrTiO_4$ thin films on Si substrate, J. Appl. Phys. 38 (1) (2005) 41–50.
[15] W.X. Cheng, A.L. Ding, P.S. Qiu, X.Y. He, X.S.H. Zheng, Optical and dielectric properties of ($Zr_{0.8}Sn_{0.2}$)$TiO_4$ thin films prepared by sol–gel process, Mater. Sci. Eng. B99 (1/3) (2003) 382–385.
[16] Y.S. Ho, M.H. Weng, S.S. Wang, High quality microwave $Zr_{0.8}Sn_{0.2}TiO_4$ dielectric thin film prepared by sol–gel method, Jpn. J. Appl. Phys. 44 (7A) (2005) 5125–5128.
[17] M. Schultz, Diffraction for Materials Scientists, Prentice–Hall Englewood Cliffs, 1982 226.
[18] F. Engelmark, J. Westlinder, G.F. Iriarie, I.V. Katardjiev, J. Olsson, Electrical characterization of AlN MIS and MIM structures, IEEE Electron Device Lett. 50 (5) (2003) 1214–1219.
[19] M. Sze, Conduction processes in insulators, in: Phys. Semicond. Devices, 2nd ed., John Wiley & Sons, New York, 1981, 403.
[20] W.J. Zhu, T.P. Ma, T. Tamagawa, J. Kim, Y. Di, Current transport in metal/hafnium oxide/silicon structure, IEEE Electron Device Lett. 23 (2) (2002) 97–99.